

Representation of Plot-Scale Soil Heterogeneity in Dual-Domain Effective Flow and Transport Models with Mass Exchange

Vilim Filipović, Yves Coquet, Horst Gerke

▶ **To cite this version:**

Vilim Filipović, Yves Coquet, Horst Gerke. Representation of Plot-Scale Soil Heterogeneity in Dual-Domain Effective Flow and Transport Models with Mass Exchange. Vadose Zone Journal, 2019, 18 (1), 14 p. 10.2136/vzj2018.09.0174 . insu-02163178

HAL Id: insu-02163178

https://insu.hal.science/insu-02163178

Submitted on 3 Jul 2019

HAL is a multi-disciplinary open access archive for the deposit and dissemination of scientific research documents, whether they are published or not. The documents may come from teaching and research institutions in France or abroad, or from public or private research centers.

L'archive ouverte pluridisciplinaire **HAL**, est destinée au dépôt et à la diffusion de documents scientifiques de niveau recherche, publiés ou non, émanant des établissements d'enseignement et de recherche français ou étrangers, des laboratoires publics ou privés.



Distributed under a Creative Commons Attribution - NonCommercial - NoDerivatives 4.0 International License

Published May 3, 2019

Special Section: Nonuniform Flow across Vadose Zone Scales

Core Ideas

- The heterogeneity of soil hydraulic properties can be described with effective parameters.
- Increasing model complexity can be used to represent plot-scale soil heterogeneity.
- One-dimensional dual-domain flow models are used to reproduce 2D preferential transport.
- Local subscale variability effects are included as mass transfer in an effective model.

Representation of Plot-Scale Soil Heterogeneity in Dual-Domain Effective Flow and Transport Models with Mass Exchange

Vilim Filipović,* Yves Coquet, and Horst H. Gerke

Agricultural soils are characterized by a structure that is strongly dependent on farming practices like tillage and trafficking. These practices can create compacted zones in the soil, thus initiating preferential flow. Two- or three-dimensional models can be used to account for the spatial variability of the soil hydraulic and transport properties. Since it is challenging to obtain such data, it is logical to find simpler approaches. Our objective was to design a one-dimensional (1D) modeling approach that effectively accounts for plot-scale soil structure variability. A 1D dual-permeability model was tested in which compacted soil was represented by a matrix domain and uncompacted soil by a fracture domain and eventually by assuming an additional immobile water region (MIM) in the fracture domain representing compacted clods embedded within the uncompacted soil. Models (1D) were compared with two-dimensional single-porosity (2D_SP) modeling results for water flow and Br^- transport based on a previously performed field tracer experiment. Results indicated good agreement between 1D dual-domain approaches (1D_DPERM and 1D_DPERM_MIM) and the 2D_SP representative model simulation results with high model efficiency and with respect to the field observations. This implied that a 1D vertical model description was sufficient to represent plot-scale variability if smaller scale soil structure heterogeneities could be accounted for as effective parameters in dual-domain models. Variation in the mass transfer term had a large effect on the vertical Br^- profile distribution. The parameters describing the sizes and shapes of the domains were most relevant for estimating mass transfer between soil structural features in heterogeneous agricultural fields. Still, the calibration of the upscaling approach of two-domain interactions in larger scale models remains challenging.

Abbreviations: 1D, one-dimensional; 1D_DPERM, one dimensional dual permeability model; 1D_DPERM_MIM, one-dimensional dual permeability model with mobile–immobile zones; 2D, two-dimensional; 2D_SP, two-dimensional single porosity model; MIM, mobile–immobile; NSE, Nash–Sutcliffe model efficiency coefficient; RMSE, root mean square error; TDR, time-domain reflectometer.

V. Filipović, Dep. of Soil Amelioration, Faculty of Agriculture, Univ. of Zagreb, 10000 Zagreb, Croatia; Y. Coquet, UMR 7327 ISTO Univ. d'Orléans, CNRS-INSU, BRGM, 45100 Orléans, France; Y. Coquet, UMR 1402 ECOSYS INRA, AgroParisTech, 75231 Paris, France; H.H. Gerke, Working Group "Hydropedology," Research Area 1 "Landscape Functioning," Leibniz Centre for Agricultural Landscape Research (ZALF), Eberswalder Straße 84, 15374 Müncheberg, Germany. *Corresponding author (vfilipovic@agr.hr).

Received 15 Sept. 2018.
Accepted 27 Jan. 2019.

Citation: Filipović, V., Y. Coquet, and H.H. Gerke. 2019. Representation of plot-scale soil heterogeneity in dual-domain effective flow and transport models with mass exchange. Vadose Zone J. 18:180174. doi:10.2136/vzj2018.09.0174

© 2019 The Author(s). This is an open access article distributed under the CC BY-NC-ND license (http://creativecommons.org/licenses/by-nc-nd/4.0/).

To understand the processes of water flow and contaminant transport in agricultural soils, models have been developed that can mechanistically describe flow, transport, and crop water and nutrient uptake. Because agricultural soils (top horizon) are constantly changing due to a large variety of tillage practices, the task of describing such complex processes is still difficult and needs to account for the temporal and spatial variability of model parameters (Green et al., 2003). Soil heterogeneities related to tillage (Petersen et al., 2001) and compaction by agricultural machinery wheels (Mohanty et al., 1994; Gysi et al., 1999) could explain the spatial variability of soil hydraulic properties (Schneider et al., 2009), solute behavior (Coquet et al., 2005a), and pesticide fate (Vieublé-Gonod et al., 2009). Soil heterogeneity is especially visible at the field scale, and therefore modeling at such scale using simple one-dimensional (1D) models does not provide a suitable explanation in every case (Ellsworth and Jury, 1991; Mayer et al., 1999).

Soil heterogeneity in natural soils in the vertical direction is mostly due to the presence of different soil horizons, which are related to soil type (Vanderborght et al., 2001; Jacques et al., 2002). In such cases, transport processes can be described using 1D models. Generally, it is assumed that water flux and storage in the unsaturated zone can be

adequately modeled by the classical Richards equation. However, due to the large spatial heterogeneity of agricultural soils, the description of soil hydraulic properties needed for vadose zone flow models is challenging. The heterogeneity of agricultural soils is characterized by variations in texture, structure, boundaries, and hydraulic conductivity (Zhang et al., 2004), among other properties. Transport processes in heterogeneous soils can be described and explained using two- or three-dimensional models, which can account for spatial variability. However, such simulations require detailed descriptions of spatial heterogeneity (e.g., Filipović et al., 2016), which are not always available and can be impractical to implement. Thus, the question arises whether 1D models can be used to account for the lateral spatial variability that may be observed at the field scale, for instance in 2D vertical soil profile cross-sections (e.g., Coquet et al., 2005a).

Another argument for reducing model dimensionality is that crop models do not explicitly account for soil structure heterogeneities, as they are generally constrained to one dimension and therefore consider only one set of soil hydraulic parameters (i.e., a single soil profile). In a way, this single set of parameters may be viewed as a set of effective or equivalent parameters (Jensen and Refsgaard, 1991; Smith and Diekkrüger, 1996). The concept of effective or equivalent soil hydraulic parameters has been mostly dealt with in upscaling procedures. Vereecken et al. (2007) reviewed upscaling methods for deriving large-scale fluxes based on small-scale soil hydraulic properties, such as stochastic perturbation methods, the stream-tube approach, and inverse modeling techniques. In addition to the upscaling issue, there is also a demand for reducing the complexity of simulation models while maintaining the validity of simulation results. The reduction of spatial dimensionality (e.g., from two to one dimension) is one way by which the complexity of models can be reduced because two dimensions can be redundant if a 1D representation is sufficient (Wang et al., 2003). In another example, Guswa and Freuberg (2002) explored the possibility of using a 1D model for describing solute spreading in a three-dimensional hydrogeologic environment with low-permeability lenses. They found that a 1D macroscopic advective–dispersive equation well matched the results from a 2D model when the equivalent conductivity of the 1D domain was less than the geometric mean of the hydraulic conductivity of the 2D domain. Therefore, reducing dimensionality may lead to changes in parameter values. The applicability of the simplified model may also be limited to specific initial and boundary conditions.

In a recent review, Vereecken et al. (2016) stated that one of the key challenges in modeling soil processes is the application of different upscaling methods to derive effective parameters and equations that allow us to include pore- and local-scale process understanding so we can describe processes at the field scale and beyond. They also discussed whether local-scale model complexity matters for prediction at a larger scale, since the large temporal and spatial resolution for measurements in the vadose zone is difficult and expensive to obtain. An important local-scale process is preferential flow, in which water and solutes move along preferred pathways (e.g., macropores) while bypassing most of the soil porous matrix (Gerke, 2006). This type of flow is responsible for local variations and nonequilibrium conditions in pressure head, water content, and solute concentration. Preferential flow pathways in agricultural soils are mainly identified as earthworm burrows, decayed root channels, and interconnected networks of cracks and fissures (e.g., Gerke, 2006). The presence of highly compacted clods, originating from trafficking, with lower permeability than the rest of the tilled layer, can trigger preferential flow as found by Coquet et al. (2005a). They found that the compacted clods embedded in the tilled layer caused water to diverge from low-permeability zones, thus creating a funneled-type heterogeneous flow velocity field. The problem was handled using a detailed soil profile description and a large data set in combination with a 2D single- porosity model and by estimating different hydraulic and transport properties for each type of soil zone (compacted vs. non-compacted).

Preferential flow can be described with two-region or even multi-region approaches to explain physical nonequilibrium of water flow and solute transport (Gerke and van Genuchten 1993a). Major challenges in dual- or multi-domain model applications are linked with the large number of parameters, which are relatively difficult to measure or estimate (Jarvis, 2007; Moeys et al., 2012). This is especially the case for the mass transfer term between the fracture and matrix regions, which depends on structure geometries, hydraulic and transport properties of aggregates and biopores, and burrow walls or clay and organic coatings. The exchange coefficient is strongly influenced by the matrix–fracture interface, which can vary in hydraulic (Gerke and Köhne, 2002) and diffusion properties (Köhne et al., 2002) but also in sorption properties such as in the case of macropore walls (Hansen et al., 1999) and in relation to organic matter composition (Ellerbrock and Gerke, 2004).

The objective of the work presented here was to design a simplified 1D model approach that effectively accounts for plot-scale soil structure variability generated by agricultural practices. Most upscaling procedures (e.g., geostatistical or Miller and Miller scaling approaches as discussed by Vereecken et al. [2007]) assume equilibrium conditions. We wanted to find an appropriate method that considers local non-equilibrium processes. As a test case for a soil plot with the type of management- and traffic-induced subscale heterogeneity, we selected the experiment performed by Coquet et al. (2005a). Our idea was to consider the highly compacted zones (below the wheel tracks) described by Coquet et al. (2005a) as the matrix domain and the more permeable soil of the inter-wheel region as the highly conductive fracture domain. This was achieved by using 1D dual-permeability model (1D_DPERM). The presence of compacted clods embedded in the tilled soil horizon between the wheel tracks was further modeled by additionally applying the mobile–immobile concept to the fracture domain (1D_DPERM_MIM) representing subscale heterogeneity. For the single- and dual-domain analyses, the HYDRUS software suite

was selected because models of different complexity can be implemented in an easily comparable way (Šimůnek et al., 2016).

Materials and Methods

Conceptual and Numerical Modeling Approaches

The conceptual approach of representing plot-scale soil heterogeneity is based on the idea that the soil plot could be described as a dual-permeability system. In this concept, compacted soil (wheel-track areas) is the matrix flow domain and more permeable soil (inter-wheel region) is the highly conductive fracture flow domain (Fig. 1). This approach was complemented by considering the fracture domain as a mobile–immobile water (MIM) dual flow system. The MIM system accounts for the compacted clods embedded in the relatively loose tilled soil horizon (Fig. 1b). Application of an effective 1D flow and transport model with increasing complexity is used to replace subscale spatial heterogeneity of transport properties. Field-scale processes may be explained with an assembly of 1D columns (e.g., Monte Carlo type of simulations), where field heterogeneity is included by varying the hydraulic and domain-specific parameters, while in the case presented here, the subscale heterogeneity (compacted clods) is also included.

The 2D numerical simulations were reproduced with the setup and parameters taken from Coquet et al. (2005b) using the single-porosity (2D_SP) model approach. Numerical simulations of 2D water flow and solute transport in variably saturated soil were performed with HYDRUS-2D, Version 2.05.0250 (Šimůnek et al., 2016). For all single- and dual-domain analyses, the HYDRUS software was selected because models with different complexity have been implemented in a consistent manner. Water flow is modeled using Richards' equation for an isotropic medium:

$$\frac{\partial \theta}{\partial t} = \frac{\partial}{\partial x}\left[K(h)\frac{\partial h}{\partial x}\right] + \frac{\partial}{\partial z}\left[K(h)\frac{\partial h}{\partial z} + K(h)\right] \quad [1]$$

where θ is volumetric water content [$L^3\ L^{-3}$], h is soil water pressure head [L], x and z are spatial coordinates in the horizontal and vertical directions, respectively [L], t is time [T], and K is the unsaturated hydraulic conductivity function [$L\ T^{-1}$].

The 2D solute transport was modeled using the Fickian-based advection–dispersion equation:

$$\frac{\partial(\theta c)}{\partial t} = \frac{\partial}{\partial x}\left(\theta D_x \frac{\partial c}{\partial x}\right) + \frac{\partial}{\partial z}\left(\theta D_z \frac{\partial c}{\partial z}\right) - \left[\frac{\partial(q_x c)}{\partial x} + \frac{\partial(q_z c)}{\partial z}\right] \quad [2]$$

where c is the solute concentration in the liquid phase [$M\ L^{-3}$], q_x and q_z represent the volumetric flux density in the horizontal and vertical directions, respectively [$L\ T^{-1}$], and D_x and D_z are the dispersion coefficients [$L^2\ T^{-1}$] for the liquid phase in the horizontal and vertical directions of the isotropic soil, described as

$$\theta D_i = D_L |q_i| + \theta D_w \tau_w \quad [3]$$

where D_L is the longitudinal dispersivity [L] along the flow direction, $|q_i|$ is the absolute value of the water flux density [$L\ T^{-1}$] in the ith direction ($i = x, z$), D_w is the molecular diffusion coefficient in free water [$L^2\ T^{-1}$], and τ_w is a tortuosity factor in the liquid phase (dimensionless), here described as a function of the pore water saturation [$\theta^{7/3}/\theta_s^2$].

Soil hydraulic functions $\theta(h)$ and $K(h)$ were described with the van Genuchten–Mualem model as

$$\theta(h) = \theta_r + \frac{\theta_s - \theta_r}{\left(1 + |\alpha_{vG} h|^n\right)^m} \quad \text{for } h < 0 \quad [4a]$$

$$\theta(h) = \theta_s \quad \text{for } h \geq 0 \quad [4b]$$

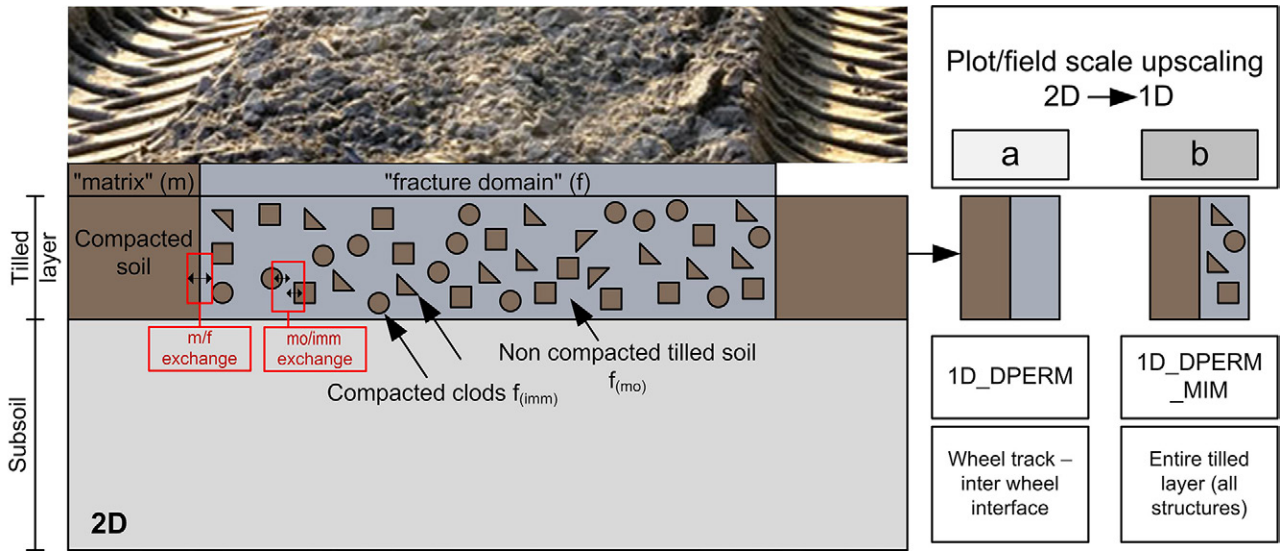


Fig. 1. A schematic two-dimensional vertical cross-section of an agricultural soil showing the compacted zones, the representative domains, mass exchange between them, and the modeling concepts for (a) a one-dimensional dual permeability model (1D_DPERM) and (b) a one-dimensional dual-permeability model with mobile–immobile zones in the fracture region [1D_DPERM_MIM; $f_{(imm)}$ and $f_{(mo)}$].

$$S_e(h) = \frac{\theta(h) - \theta_r}{\theta_s - \theta_r} \quad [5]$$

$$K(h) = K_s S_e^{0.5} \left[1 - \left(1 - S_e^{1/m}\right)^m\right]^2 \quad [6]$$

where θ_r and θ_s denote residual and saturated volumetric water content, respectively, K_s is the saturated hydraulic conductivity [L T^{-1}], S_e is effective saturation (dimensionless), α_{vG} [L^{-1}] and n (dimensionless) are shape parameters ($n > 1$), and $m = 1 - 1/n$. A modified van Genuchten-type function with an air-entry value of −2 cm (Vogel et al., 2000b) was used in the 2D simulations to prevent numerical instability.

In the 1D dual-permeability modeling approach (1D_DPERM), compacted soil under the wheel tracks was treated as "matrix" (subscript *m*) and non-compacted soil between the wheel tracks as "fracture" domain (subscript *f*), with a mass exchange term to connect the domains (Fig. 1a). The dual-permeability model (Gerke and van Genuchten, 1993a) assumes two mobile pore domains with separate flow and transport properties assigned to each. The coupled set of two Richards' equations is described (Šimůnek et al., 2016) as

$$\frac{\partial \theta_f(h_f)}{\partial t} = \frac{\partial}{\partial z}\left[K_f(h_f)\left(\frac{\partial h_f}{\partial z} + 1\right)\right] - \frac{\Gamma_w}{w} \quad [7]$$

$$\frac{\partial \theta_m(h_m)}{\partial t} = \frac{\partial}{\partial z}\left[K_m(h_m)\left(\frac{\partial h_m}{\partial z} + 1\right)\right] + \frac{\Gamma_w}{1-w} \quad [8]$$

where w is the volume ratio of the fracture domain (dimensionless). Note that the water content of the bulk soil, θ, is separated into the local water contents, θ_f and θ_m, of the pore domains by $\theta = w\theta_f + (1 - w)\theta_m$. In a similar way, the bulk soil water flux density, q [L T^{-1}], is defined as $q = wq_f + (1 - w)q_m$. Following Gerke and van Genuchten (1993b), the water transfer term Γ_w [T^{-1}] is

$$\Gamma_w = \alpha_w(h_f - h_m) \quad [9]$$

in which α_w is a first-order mass transfer coefficient [L^{-1} T^{-1}] for water flow, defined as

$$\alpha_w = \frac{\beta}{a^2}\gamma_w K_a(h) \quad [10]$$

where β is a geometry-dependent coefficient (dimensionless), a is the characteristic length of the matrix structure [L], $\gamma_w = 0.4$ is a scaling coefficient (dimensionless), and K_a is the effective hydraulic conductivity of the fracture–matrix interface [L T^{-1}], here taken as the matrix hydraulic conductivity function, $K_a(h) = K_m(h)$, with the saturated value, $K_{a,s} \leq K_{m,s}$, and calculated as the arithmetic mean of the values evaluated at the domains' pressure head:

$$K_a(h) = 0.5\left[K_a(h_f) + K_a(h_m)\right] \quad [11]$$

The dual-permeability formulation for solute transport is based on two coupled advection–dispersion equations (Gerke and van Genuchten, 1993a):

$$\frac{\partial \theta_f c_f}{\partial t} = \frac{\partial}{\partial z}\left(\theta_f D_f \frac{\partial c_f}{\partial z}\right) - \frac{\partial q_f c_f}{\partial z} - \frac{\Gamma_s}{w} \quad [12]$$

$$\frac{\partial \theta_m c_m}{\partial t} = \frac{\partial}{\partial z}\left(\theta_m D_m \frac{\partial c_m}{\partial z}\right) - \frac{\partial q_m c_m}{\partial z} + \frac{\Gamma_s}{1-w} \quad [13]$$

where Γ_s is the solute mass transfer term [M L^{-3} T^{-1}] (Gerke and van Genuchten, 1996):

$$\Gamma_s = \alpha_s^{DPERM}(1-w)\theta_m(c_f - c_m) + \Gamma_w c^* \quad [14]$$

where c^* is either c_f or c_m depending on the exchange direction, and α_s^{DPERM} is the first-order solute mass transfer rate coefficient [T^{-1}] of the form

$$\alpha_s^{DPERM} = \frac{\beta}{a^2} D_a \quad [15]$$

in which D_a is an effective diffusion coefficient [L^2 T^{-1}] that represents the diffusion properties of the fracture–matrix interface (e.g., accounting for organic coatings).

In a second 1D_DPERM model (Fig. 1b), the compacted clods embedded in the tilled soil between the wheel-track compaction zones were separately considered in the solute transport model by using the mobile–immobile water model (MIM) concept. Here, the immobile pore water region in the clods is interacting via first-order mass exchange with the surrounding non-compacted soil of the fracture domain. This dual-permeability mobile–immobile model (1D_DPERM_MIM) assumes that the water content and the solute mass in the fracture domain (i.e., analogously to Šimůnek and van Genuchten [2008] for the matrix domain) is partitioned into mobile (flowing), $\theta_{f,mo}$ [L^3 L^{-3}], and immobile (stagnant), $\theta_{f,im}$ [L^3 L^{-3}], components assuming local equilibrium in the pressure head:

$$\theta_f = \theta_{f,mo} + \theta_{f,im}$$

and

$$c_f\theta_f = c_{f,mo}\theta_{f,mo} + c_{f,im}\theta_{f,im} \quad [16]$$

Allowing for non-equilibrium in solute transport, the governing set of convection–dispersion equations for transport in the fracture region, Eq. [11], is then replaced (Šimůnek and van Genuchten, 2008) by

$$\frac{\partial \theta_f c_{f,mo}}{\partial t} + \frac{\partial \theta_f c_{f,im}}{\partial t} = \frac{\partial}{\partial z}\left(\theta_f D_f \frac{\partial c_{f,mo}}{\partial z}\right) - \frac{\partial q_f c_{f,mo}}{\partial z} - \frac{\Gamma_s}{w} - \Gamma_s^* \quad [17]$$

$$\frac{\partial \theta_f c_{f,im}}{\partial t} = \Gamma_s^* = \alpha_s^{MIM}\left(c_{f,mo} - c_{f,im}\right) \quad [18]$$

where $c_{f,mo}$ and $c_{f,im}$ denote solute concentrations in the mobile and immobile regions of the fracture domain [M L^{-3}], respectively, and α_s^{MIM} is a first-order exchange term for the mobile–immobile model [T^{-1}].

Experimental Field Data and Modeling Setup

The experimental data used in this study were published by Coquet et al. (2005a, 2005b). The field experiment was performed at the INRA experimental station in Grignon (8°50′49″ N, 1°56′49″ E) on a Calcic Cambisol (FAO classification). It was conducted to explore the impact of soil structure heterogeneity due to trafficking and tillage on water and solute transport. The experiment was performed on a 4- by 2-m field plot using a rainfall simulator and Br^- (tracer) solution. First, the plot was irrigated with water (21 mm h^{-1}) for 4 h and 20 min (4.5 h time period was used in modeling) and then Br^- solution was added (using a rainfall intensity of 26 mm h^{-1} for 2 h). Twelve hours after the tracer infiltration, a whole profile (3 m wide and 0.66 m deep) was sampled with small cores (4 cm in diameter and 2 cm in height) and analyzed to produce a 2D Br^- distribution map. Soil water contents (TDRs) and pressure heads (tensiometers) were monitored at specific locations corresponding to compacted soil below wheel tracks, compacted clods, and non-compacted soil in between wheel tracks (Fig. 2a). Thirty TDR probes (20 cm long) and 30 mini-tensiometers (2 cm long, 0.6-cm outside diameter on

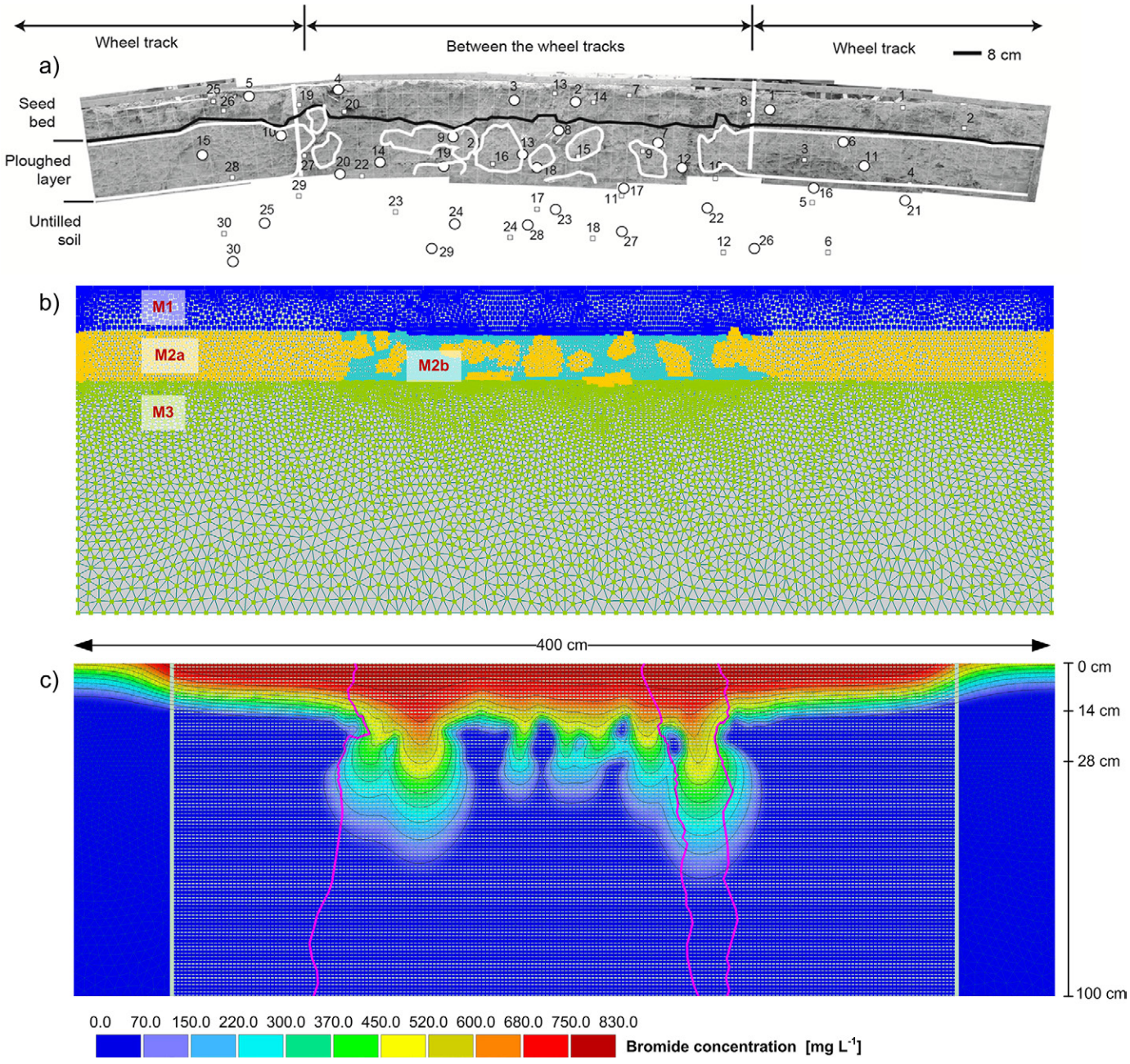


Fig. 2. (a) Soil pit field description and experimental setup with locations of time-domain reflectometer (TDR) probes (white circles) and tensiometers (white squares) (Coquet et al., 2005a), (b) two-dimensional (2D) material distribution (M1, seed bed; M2a, compacted material; M2b, non-compacted material; M3, subsoil), and (c) 2D numerical reproduction of the heterogeneous Br^- concentration plume (T = 20 h, Coquet et al., 2005b) with horizontal cross-section mesh (n = 101, white lines) and vertical irregular mesh lines (x = distance from left: 85, 175, and 195 cm, pink lines) taken for the comparison with one-dimensional simulations.

80-cm-long polyvinyl chloride tubes) were installed to monitor the soil water dynamics within the tilled soil. However, after data collection, one TDR probe and eight tensiometers were found to give unreliable results and were excluded from the data set. The field data showed that the compacted soil zones with low hydraulic conductivity values limited the penetration depth of Br^- (Coquet et al., 2005a). In a second step, water and Br^- transport were successfully reproduced by numerical modeling with HYDRUS-2D using a fully deterministic approach using measured areas of the compacted regions for describing the soil structure heterogeneity (Coquet et al., 2005b). Water flow and solute transport were simulated for a rectangular domain, 300 cm wide and 100 cm deep, with a triangular mesh of 16,145 elements, with the smallest elements close to the soil surface. Initial conditions for water flow from measured pressure heads were set to values of −225 cm at the bottom of the tilled layer and for the entire third soil horizon (Fig. 2b) and −500 cm at the soil surface, with a linear distribution in the tilled layer. Simulation was started 13 h before the first irrigation event. An atmospheric boundary condition was imposed at the top and free drainage at the bottom of the soil profile.

The results from the 2D modeling presented by Coquet et al. (2005b) were used in this study for comparison with the 1D modeling in which soil structure heterogeneity is accounted for by increasing model complexity (dual-permeability 1D_DPERM and dual-permeability with mobile–immobile model 1D_DPERM_MIM). The 1D modeling was set up as close as possible to the 2D simulations, having the same initial and boundary conditions and the same parameter values for those that do not have a dimensionality difference. The soil water dynamics and tracer concentrations (Br^-) simulated for the duration of the field experiment (37 h) with the 1D effective flow models were compared with the results of the 2D modeling. To compare the results of both simulations, 2D results for water content and solute mass (with respect to the averaged water content) distribution were averaged across the lateral dimension at selected depths. At selected times (19.5, 20, 22.5, 25, 27.5, 30, 31.5 and 37 h), 2D horizontal cross-section charts were reproduced with a 1-cm depth resolution and compared with the 1D model results from the soil surface down to the 100-cm depth (101 charts). At each depth of the 2D simulations, average values of water content and solute mass were calculated using the corresponding chart (Fig. 2c, white dense grid).

In the 1D simulations, mass transfer rates were calculated in HYDRUS-1D as mass transfer between matrix and fracture domains, while in HYDRUS-2D "mesh lines" were inserted at the location where we visually found the best-suited distribution in the second layer between compacted (matrix) and non-compacted (fracture) regions (e.g., $x = 85$ cm, Fig. 2c). Mass transfer rates were derived from water and solute flux data across the selected lines.

Soil hydraulic parameter values were measured by Coquet et al. (2005a). They were derived from field and laboratory measurements (tension-disk infiltrometry, constant-head method, evaporation method, and pressure plates), while additional fine tuning was necessary to be able to effectively simulate field water and Br^- distribution (Coquet et al., 2005b). To describe the sensor data (TDRs and tensiometers) and Br^- concentration profiles, additional fitting was performed using the HYDRUS-2D inverse optimization procedure, which resulted in a relatively good fit with field observations (Table 1). In the dual-flow modeling approach, the parameters for Material 1 and Material 3 were the same for the matrix and the fracture regions, while Material 2 had different fracture and matrix parameters and was divided into Material 2a and Material 2b (M2a was compacted soil and M2b was non-compacted soil). In the 1D_DPERM_MIM model, the immobile water content $\theta_{s,f,im}$ was 0.07 $cm^3\ cm^{-3}$, thus reducing the $\theta_{s,f,mo}$ of the fracture region to 0.32 $cm^3\ cm^{-3}$ (Table 2). The n parameter for M2a, M2b, and M3 was fixed to a value of $n = 1.2$ (for M2a, M2b, and M3 horizons) to avoid numerical problems during the simulation (e.g., Ippisch et al., 2006).

Parameter w (dimensionless) was estimated by evaluating the proportion of non-compacted vs. compacted soil in the middle layer, while the $K_{a,s}$ value and the mass transfer coefficients for water, α_w, and solutes, α_s^{DPERM} and α_s^{MIM}, were selected as proposed previously (e.g., Gerke et al., 2013; Haws et al., 2005). Additional transport parameters for the differently complex models are presented in Table 2. Furthermore, sensitivity analyses of water and solute mass transfer parameters were performed to analyze their effects on the vertical distributions of Br^- concentrations in the soil.

The fitting of the 1D modeling was evaluated by comparing the results with the reference 2D simulation of water and Br^- distributions (Coquet et. al., 2005b) and by comparing both

Table 1. Soil hydraulic parameters of residual and saturated water content (θ_r and θ_s, respectively), saturated hydraulic conductivity (K_s), and van Genuchten α_{vG} and n parameters used for the 1D_DPERM and 1D_DPERM_MIM models based on inverse optimization using time-domain reflectometry and tensiometer data observed in the field plot, here from 2D_SP model optimization (Coquet et al., 2005b). In one-dimensional modeling, the properties were attributed to matrix and fracture domains separately while in two dimensions, M2a and M2b were modeled as two different materials within this soil horizon.

Depth and description	θ_r	θ_s	α_{vG}	K_s	n
	$cm^3\ cm^{-3}$		cm^{-1}	$cm\ h^{-1}$	
M1_seed bed (0–12-cm layer) matrix	0.02	0.30	0.104	42.2	1.6
M1_seed bed (0–12-cm layer) fracture	0.02	0.30	0.104	42.2	1.6
M2a_compacted material (13–29-cm layer) matrix	0.00	0.39	0.00287	0.1	1.2
M2b_non-compacted material (13–29-cm layer) fracture	0.00	0.38	0.0752	24.4	1.2
M3_subsoil (30–100-cm layer) matrix	0.06	0.38	0.107	29.6	1.2
M3_subsoil (30–100-cm layer) fracture	0.06	0.38	0.107	29.6	1.2

Table 2. Transport parameters used in the 2D_SP, 1D_DPERM, and 1D_DPERM_MIM models: longitudinal dispersivity (D_L), dispersivity of the matrix (D_m) and fracture (D_f) domains, molecular diffusion coefficient in water (D_w), volume ratio of fracture domain(w), geometry-dependent coefficient β, dimensionless scaling factor γ_w, the characteristic length of the matrix structure (a), the effective saturated hydraulic conductivity of the fracture–matrix interface ($K_{a,s}$), the first-order solute mass transfer rate coefficient (α_s^{DPERM}) and the first-order exchange term for the mobile–immobile model (α_s^{MIM}), the first-order mass transfer coefficient for water flow (α_w), and the immobile water content in the fracture region representing embedded clods ($\theta_{s,f,im}$).

Model	D_L	D_m	D_f	D_w	w	β	γ_w	a	$K_{a,s}$	α_s^{DPERM}, α_s^{MIM}	α_w	$\theta_{s,f,im}$
		—— cm ——		$cm^2\ h^{-1}$				cm	$cm\ h^{-1}$	h^{-1}	$cm^{-1}\ h^{-1}$	$cm^3\ cm^{-3}$
2D_SP	5	–	–	0.0675	–	–	–	–	–	–	–	–
1D_DPERM	–	5	10	0.0675	0.5	15	0.4	5	0.01	0.006	0.0024	–
1D_DPERM_MIM	–	5	10	0.0675	0.5	15	0.4	5	0.01	0.006	0.0024	0.07

Br^- simulation results with the field data. Comparisons were performed using the Nash–Sutcliffe model efficiency coefficient (NSE; Nash and Sutcliffe, 1970), the root mean square error (RMSE), and the coefficient of determination (R^2):

$$\mathrm{NSE} = 1 - \frac{\sum_{i=1}^{N}(O_i - S_i)^2}{\sum_{i=1}^{N}(O_i - \bar{O})^2} \quad [19]$$

$$\mathrm{RMSE} = \sqrt{\frac{\sum_{i=1}^{N}(O_i - S_i)^2}{N-1}} \quad [20]$$

$$R^2 = \left[\frac{\sum_{i=1}^{N}(O_i - \bar{O})(S_i - \bar{S})}{\left[\sum_{i=1}^{N}(O_i - \bar{O})^2\right]^{0.5}\left[\sum_{i=1}^{N}(S_i - \bar{S})^2\right]^{0.5}}\right]^2 \quad [21]$$

where O_i and S_i represent observed or reference and simulated values, respectively, $\bar{O}$ and $\bar{S}$ represent the averages of the observed or reference and simulated values, respectively, and N is the number of values.

Results

Comparison of One-Dimensional vs. Two-Dimensional Modeling

The simulations using 1D_DPERM and 1D_DPERM_MIM for water content matched the 2D_SP model predictions but with more slowly decreasing curves at the end of the experiment (after irrigation ceased, Fig. 3a). Rapid increase was found in water contents, approaching water saturation soon after the start of the initial irrigation at time 13 h. The largest difference between the models was observed for water content values at the 10-cm depth, where the reference 2D simulation predicted a more pronounced drying compared to the 1D simulations. Regarding the tracer movement (Fig. 3b), the Br^- concentration time series at the 10-cm depth were slightly closer to the 2D_SP model for 1D_DPERM_MIM than for 1D_DPERM because the concentration was gradually increasing for the entire period as predicted with the 2D-SP model. However, the 1D_DPERM predictions displayed a closer match with 2D simulations than the 1D_DPERM_MIM at greater depths (e.g., 30 cm), as shown by statistical performance evaluation indicators (Table 3).

Vertical profile distributions of water content and Br^- concentration (Fig. 4) revealed the largest variations in the soil plow layer, as a result of this layer having two different parameter sets in the matrix and fracture regions with large differences among hydraulic parameters (Table 1). The increase in water content was mostly connected with the relatively low K_s value (0.1 cm h^{-1}) of M2a (the compacted region under the wheel tracks) that led to an increase in water saturation during irrigation above the second layer (Fig. 3a) from 15 to 19.5 h. The 1D_DPERM_MIM model predicted lower water content in the second layer compared with 2D_SP (Fig. 4b) due to the presence of compacted clods in the fracture region. The comparison of the Br^- concentration profiles in the fracture region revealed differences between the effective 1D model approaches (i.e., more pronounced concentration increase for 1D_DPERM_MIM vs. 1D_DPERM below the plow pan at −30 cm). Additionally, field observations (Fig. 4c and 4d) revealed that both simulations (1D and 2D) were in the range of measured Br^- concentrations at selected times ($R^2_{2D_SP} = 0.95$, $R^2_{DPERM} = 0.94$, $R^2_{DPERM_MIM} = 0.88$). Although the model (2D_SP) has already been validated (Coquet et al., 2005b), the Br^- data were provided here to show that the models, indeed, reflected the field situation.

Efficiency of the 1D dual-flow models was found to be high at all selected time steps during the experiment (Table 3) compared with the 2D_SP model (NSE > 0.7, R^2 > 0.8, and RMSE < 0.03 $cm^3\ cm^{-3}$ for water content), while the Br^- concentration displayed even better dual-permeability model performance (NSE > 0.9, R^2 > 0.9, and RMSE < 24 mg L^{-1}, i.e., <3% of the maximum concentration). These efficiency values demonstrate that increasing the model complexity to a dual-flow setup to match the field conditions can indeed be used to reduce dimensionality and characterize soil heterogeneity. From different sets of simulations (not shown here), it was evident that the volume of compacted soil in relation to the non-compacted region (in the 2D_SP model) plays an important role. As we increased the amount of compacted soil (matrix flow) by selecting a wider track area by decreasing the w values in Eq. [7], the importance of embedded soil clods declined and the better model performance in terms of the NSE efficiency

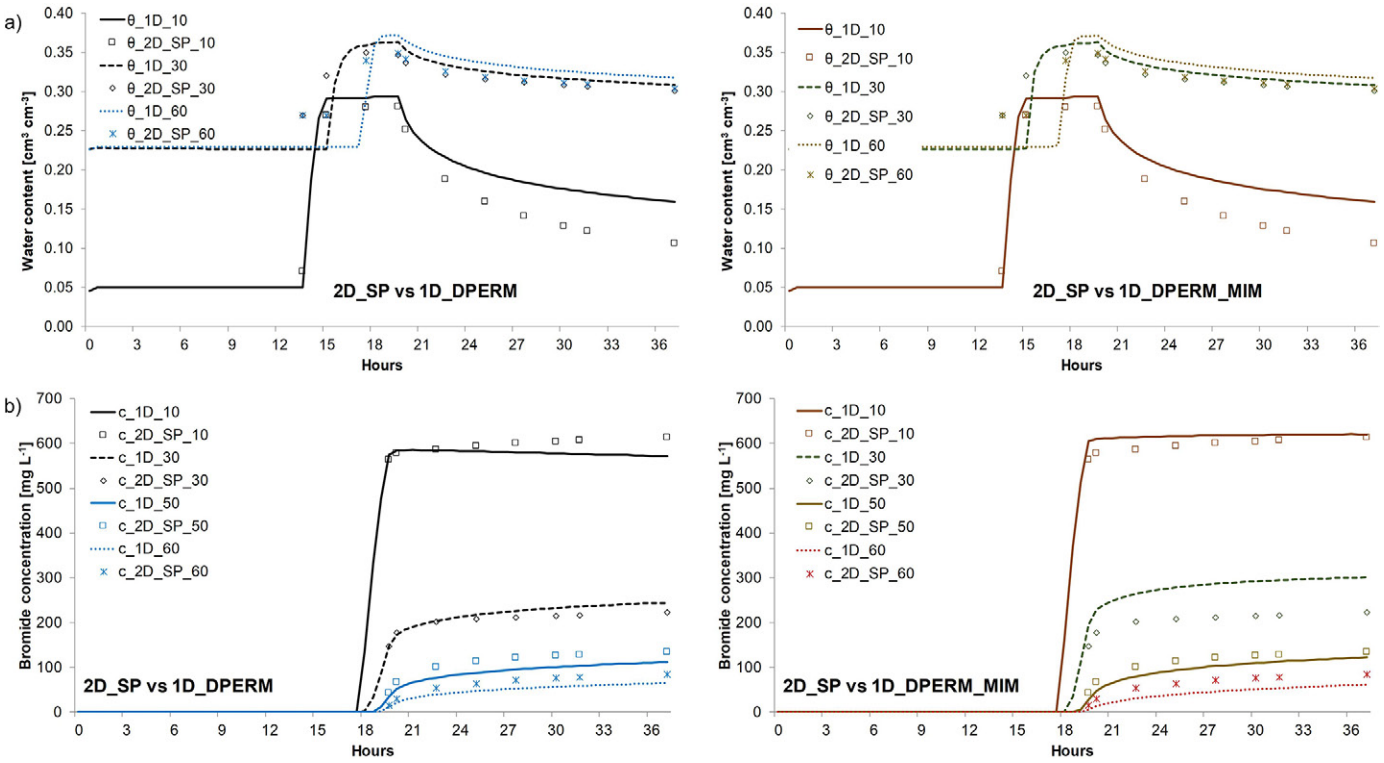


Fig. 3. Comparison of two-dimensional single-porosity (2D_SP), one-dimensional dual-permeability (1D_DPERM), and one-dimensional dual-permeability with immobile water in the fracture (1D_DPERM_MIM) models for (a) water content (θ) and (b) Br^- concentration (c) during the field experiment (irrigation started at 13 h, end time was 37 h) at selected soil depths (10, 30, 50, and 60 cm).

tended more toward the 1D_DPERM without MIM. For example, using a value of $w = 0.4$, the NSE at time 20 h for 1D_DPERM for the Br^- vertical concentration distribution was 0.92 and 0.94 for 1D_DPERM_MIM while for the last time ($T = 37$ h), NSE was 0.84 for 1D_DPERM and 0.82 for 1D_DPERM_MIM.

Mass Transfer and Its Sensitivity

The mass exchange rate between the matrix and fracture domains was estimated from the 2D_SP simulation as flux across the interface between the compacted and non-compacted soil regions; it was calculated at locations (x) by using the mesh line option in the HYDRUS code (Fig. 2c). Note that in two dimensions, the reported "mass exchange" considers all lateral flow components along a single mesh line, integrating all lateral exchanges along the line, which can provide some justification for differences in exchange fluxes between the two approaches (Fig. 5). In the 2D simulation, the water front was diverted laterally toward the central part of the domain when approaching

Table 3. Values of the Nash–Sutcliffe efficiency (NSE), the coefficient of determination (R^2), and the root mean square error (RMSE) for the comparison between two-dimensional single porosity (2D_SP) vs. one-dimensional dual-permeability (1D_DPERM) and one-dimensional dual-permeability with immobile water in the fracture (1D_DPERM_MIM) for water content (θ) and Br^- concentration (c) at different times during the simulated experiment.

	20 h		22.5 h		25 h		27.5 h		31.5 h		37 h	
2D_SP vs.	θ	c	θ	c	θ	c	θ	c	θ	c	θ	c
	$cm^3\ cm^{-3}$	$mg\ L^{-1}$	$cm^3\ cm^{-3}$	$mg\ L^{-1}$	$cm^3\ cm^{-3}$	$mg\ L^{-1}$	$cm^3\ cm^{-3}$	$mg\ L^{-1}$	$cm^3\ cm^{-3}$	$mg\ L^{-1}$	$cm^3\ cm^{-3}$	$mg\ L^{-1}$
NSE												
1D_DPERM	0.74	0.99	0.80	0.98	0.82	0.98	0.83	0.97	0.83	0.96	0.84	0.95
1D_DPERM_MIM	0.72	0.99	0.79	0.98	0.81	0.98	0.81	0.98	0.82	0.98	0.82	0.97
R^2												
1D_DPERM	0.93	0.99	0.92	0.99	0.91	0.99	0.91	0.99	0.91	0.98	0.92	0.98
1D_DPERM_MIM	0.81	0.98	0.85	0.99	0.86	0.98	0.87	0.98	0.87	0.98	0.88	0.98
RMSE												
1D_DPERM	0.02	23.7	0.02	30.1	0.03	34.7	0.03	38.6	0.03	43.3	0.03	47.5
1D_DPERM_MIM	0.02	28.1	0.03	27.3	0.03	28.8	0.03	31	0.03	34	0.03	37.1

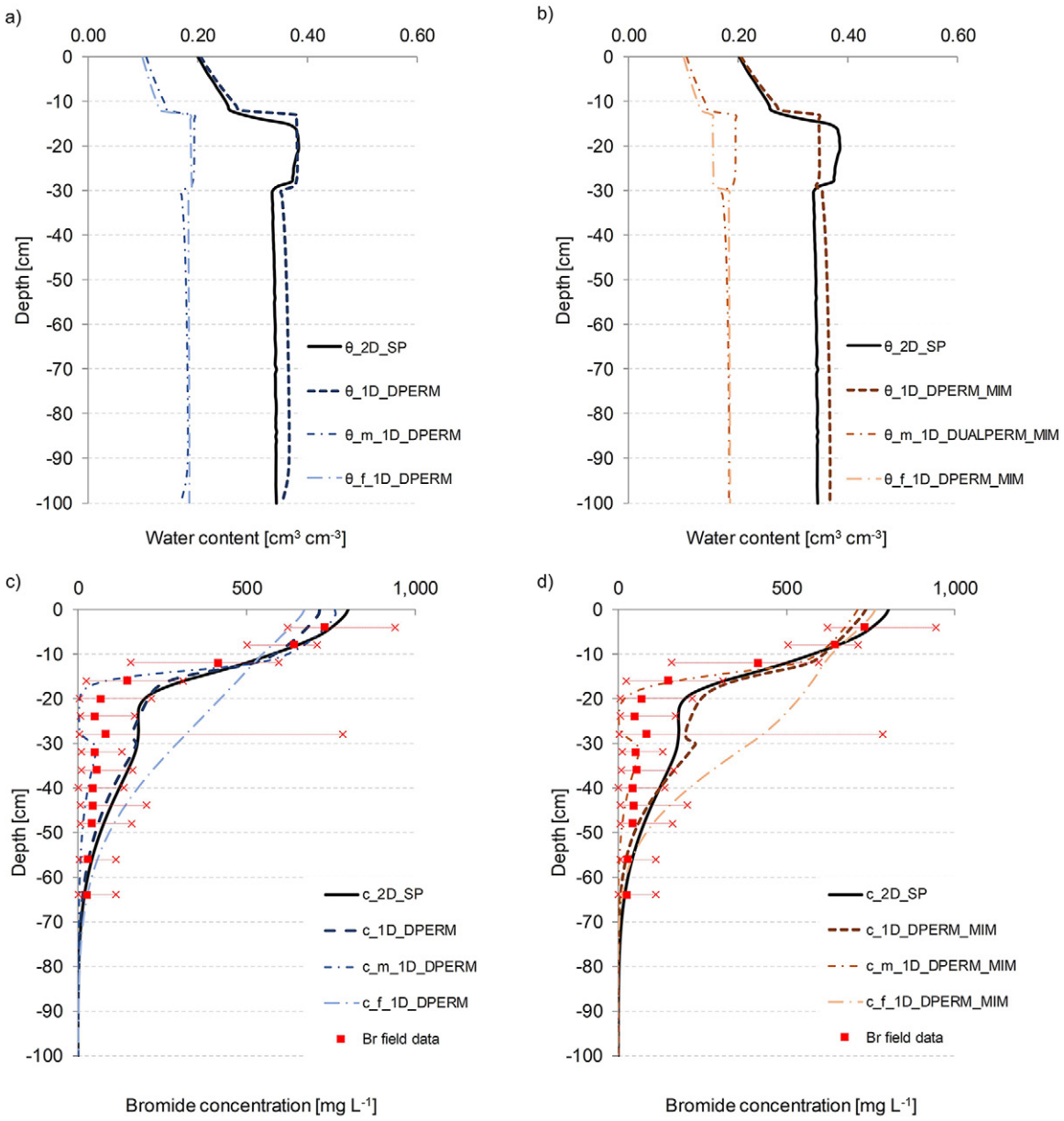


Fig. 4. Vertical profiles of (a,b) water content and (c,d) Br^- concentration simulated with the two-dimensional single-porosity (2D_SP) model and (a,c) one-dimensional dual-permeability (1D_DPERM) model or (b,d) one-dimensional dual-permeability model with mobile–immobile regions in the fracture domain (1D_DPERM_MIM) at time T = 20 h. The field Br^- concentration data (n = 20 per depth, sampling at different horizontal x spacings) are represented by red squares with indication of maximum and minimum range (red × marks).

the compacted wheel tracks located on the right and left sides of the domain (Fig. 2c). Calculations along the mesh lines show that mass transfer occurred mostly in the direction matrix → fracture (Fig. 5a). Due to irrigation-created nonequilibrium conditions, the DPERM models showed similar behavior at the beginning of irrigation (at 13 h), with exchange from the matrix to the fracture region, while later the DPERM mass exchange decreased and shifted in the other direction. The selected mesh lines in the 2D_SP model did not match at later times with the DPERM predictions, but we did not try to optimize the transfer coefficients based on these results. The effect of the mass transfer term and exchange properties between matrix and fracture in one dimension are also influencing water and Br^- flux at the bottom boundary (Fig. 5b and 5c). The water front in both 1D models was delayed for 2 h compared with 2D_SP. This indicates the importance of mass exchange parameters in dual-domain models, which sensitivity was therefore tested (see below). The discrepancy between the 2D_SP and 1D models (Fig. 5c) could also originate from the air-entry value of −2 cm used in the 2D model, which influenced solute flux (it caused a reduction of the actual surface flux under saturated conditions).

The plow layer played a major role in solute mass transfer, with the largest value found just above it during the Br^- application (850 mg L^{-1}; T = 19.5 h) from matrix to fracture regions as shown in Fig. 6, but also in the reverse direction just below. Both 1D_DPERM and 1D_DPERM_MIM reproduced similar vertical

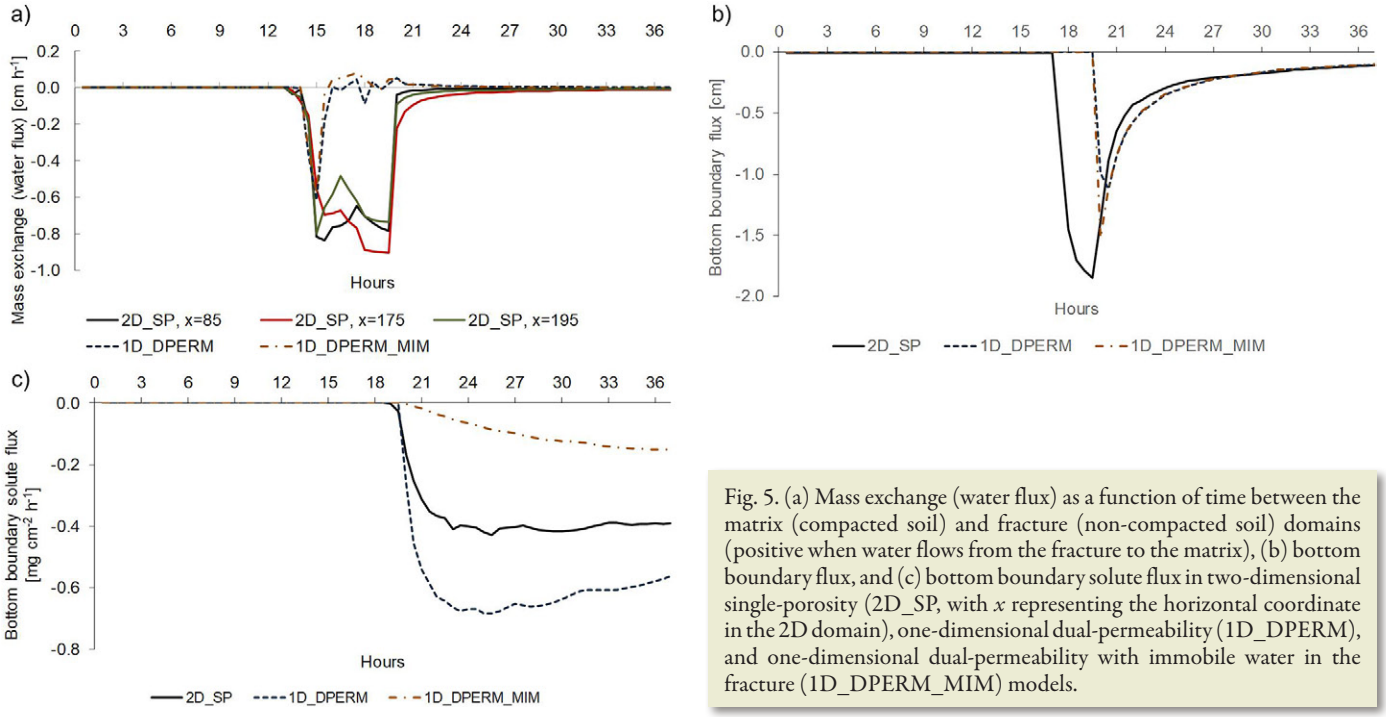


Fig. 5. (a) Mass exchange (water flux) as a function of time between the matrix (compacted soil) and fracture (non-compacted soil) domains (positive when water flows from the fracture to the matrix), (b) bottom boundary flux, and (c) bottom boundary solute flux in two-dimensional single-porosity (2D_SP, with x representing the horizontal coordinate in the 2D domain), one-dimensional dual-permeability (1D_DPERM), and one-dimensional dual-permeability with immobile water in the fracture (1D_DPERM_MIM) models.

profiles of solute mass transfer. During the nonequilibrium situation shortly after the beginning of irrigation with the Br^- solution (T = 19.5 h), the mass transfer was largest just above the plow layer (at the bottom of the seed bed) and directed as expected from the matrix into the fracture domain due to the low permeability of the matrix region in the plow layer ($K_{m,s}$ = 0.1 cm h^{-1}).

The sensitivity of the vertical Br^- distribution to the water, α_w, and solute, α_s^{DPERM} and α_s^{MIM}, mass transfer coefficients was tested (Fig. 7) for the 1D_DPERM and 1D_DPERM_MIM models. In Fig. 7, the effective hydraulic conductivity of the matrix

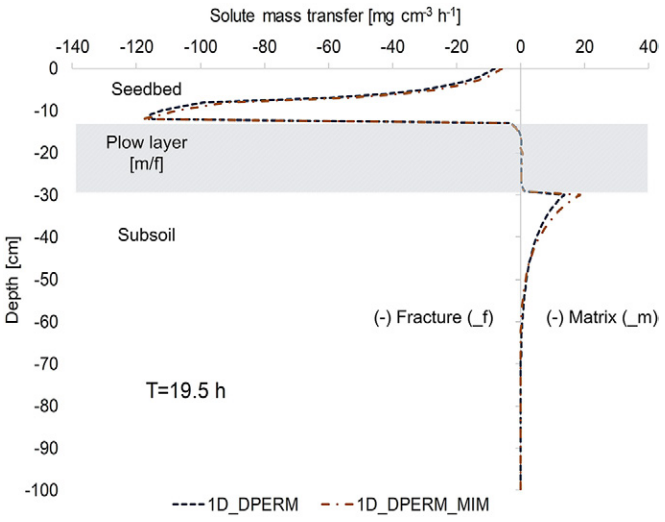


Fig. 6. Vertical distribution of the solute mass transfer rate in one-dimensional dual-permeability (1D_DPERM) and one-dimensional dual-permeability with immobile water in the fracture (1D_DPERM_MIM) models at time T = 19.5 h. Positive values of the mass transfer term indicate transfer from the fracture into the matrix domain, and negative values indicate the exchange from matrix into fracture domain.

fracture interface, $K_{a,s}$ (at 0.1, 0.01, and 0.001 cm h^{-1}) had a relatively small effect on the Br^- distribution compared with the solute transfer coefficients (0.06, 0.006, and 0.0006 h^{-1}). Similar combinations of water and solute mass transfer coefficients were used elsewhere (e.g., Gerke et al., 2013). The presented results (Fig. 6 and 7) indicate that compacted zones in the soil profile could lead to plot-scale preferential flow effects controlled by the water exchange rate between the two porous domains. However, the sensitivity of the solute mass transfer coefficients for the fixed shape and size parameters (β and a), representing the geometry of the compacted region, was different from the water transfer term coefficients.

Discussion

Spatial Dimensionality and Upscaling

The proposed effective 1D flow and transport model concept (Fig. 1) was applied here to arable soils in which soil cultivation has led to more or less compacted regions with highly contrasting hydraulic properties. At the plot scale (i.e., an area of 4–20 m^2), these heterogeneities could be spatially described in detail and included in 2D or 3D single-domain numerical models (Coquet et al., 2005b; Filipović et al., 2016). For the field scale, the explicit consideration of such details is mostly not possible, and approaches for simplification are required. One possibility after having identified repeated plot-scale structures was evaluated here. The idea was to include those structures that could lead to short-distance subplot nonequilibrium and lateral flow processes into lumped 1D plot-scale models with effective parameters. Further upscaling to obtain field-scale information could be performed with these effective plot-scale models (e.g., Cadini et al., 2012) by using Monte Carlo type simulations (e.g., Arora et al., 2015) assuming an ensemble of parallel and statistically independent plots (e.g., Mallants

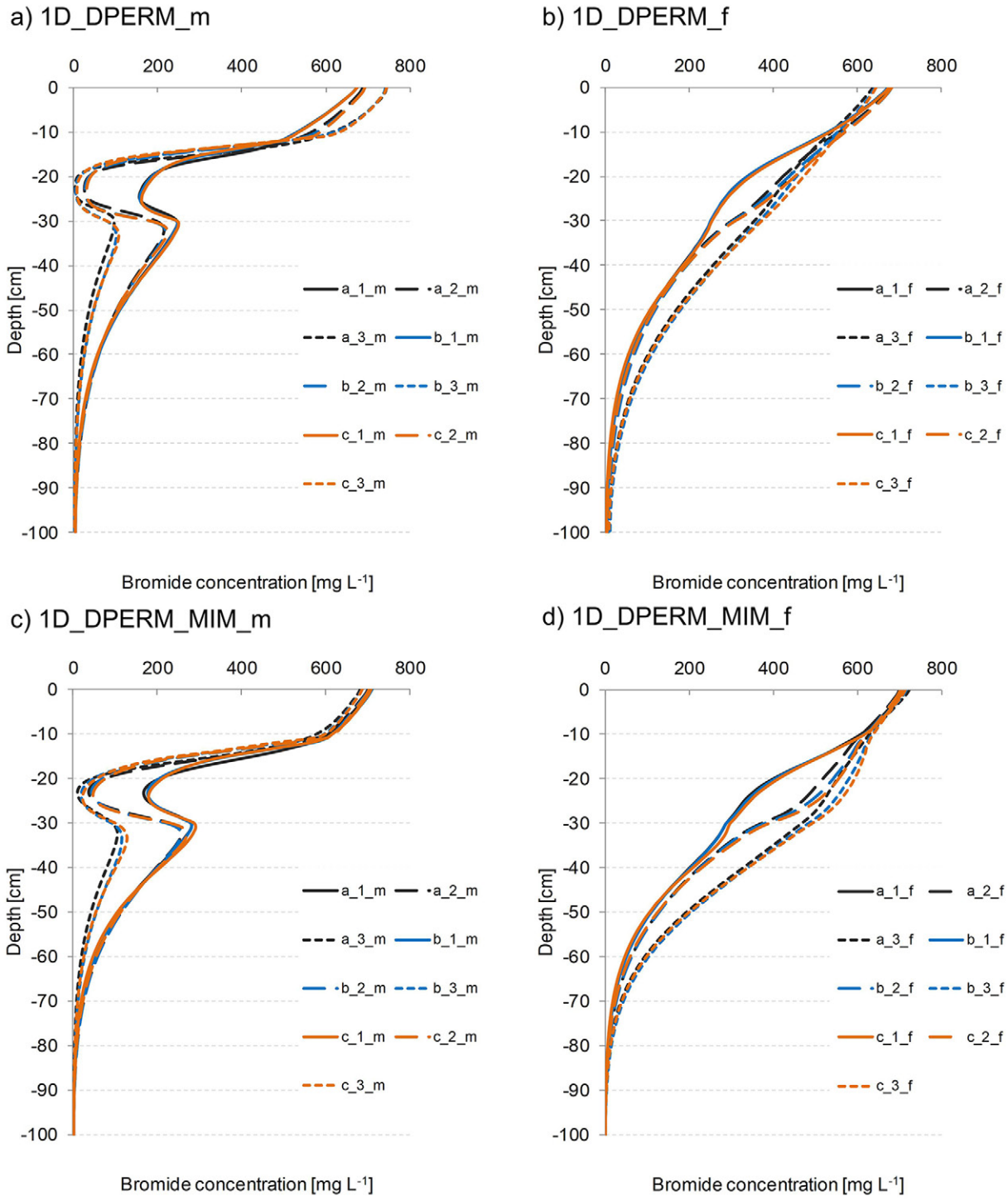


Fig. 7. Vertical distribution of the Br^- concentration at the end of the experiment (37 h) in (a,b) for the 1D_DPERM model and (c,d) for the 1D_DPERM_MIM model for matrix (_m) and fracture (_f) regions in relation to combinations of values of the water transfer rate coefficients, α_w (a: 0.024 $cm^{-1}\ h^{-1}$, b: 0.0024 $cm^{-1}\ h^{-1}$, c: 0.00024 $cm^{-1}\ h^{-1}$), and solute transfer coefficients, α_s^{DPERM} and α_s^{MIM} (1: 0.06 h^{-1}, 2: 0.006 h^{-1}, 3: 0.0006 h^{-1}).

et al., 1996) that could additionally have different hydraulic and effective parameters across the field (e.g., the distribution of compacted clods, among other properties). An additional benefit of our approach is the possibility of including local-scale heterogeneities induced by tillage and other similar soil structural features considered in the model subdomain (through MIM model addition). Other spatial averaging (e.g., Ahuja et al., 2010; Lai and Ren, 2016) and stochastic upscaling approaches (e.g., Zhu and Mohanty, 2002, 2003) to generate effective hydraulic parameters could be further used for field (and larger scales) upscaling.

The present approach covers structures at two intermediate scales: (i) compacted soil regions and large clods that can explicitly be treated in 2D macroscopic modeling and (ii) macropores created by cracks and biopores that are sub-macroscopic-scale

structures that cannot be explicitly considered. Both structures can be spatially variable (Vogel et al., 2000a) and lead to local nonequilibrium conditions when looking at the processes from the respective next larger scale. For the plot scale, the movement of water and especially that of the tracer from the more conductive soil into the compacted regions takes some time, which in the effective model is considered in the form of first-order kinetic coefficients (Fig. 7). The sub-macroscopic-scale heterogeneities (i.e., macropores) were not considered here; however, additional effects of macropores using the same first-order approach would require separate sets of exchange parameters, leading to multiple-domain modeling (e.g., Gerke, 2006).

The proposed reduction in spatial dimensionality from two or three to one dimension using a dual-region approach could be useful when trying to incorporate smaller scale effects of the soil structure on soil hydraulic processes, for instance in crop modeling. In this sense, the 1D_DPERM approach could be used to include preferential flow effects generated by agricultural practices (e.g., compaction below wheel tracks or plowing) into 1D crop models without having to increase model dimensionality. Models that can predict the amount of compacted soil in the profile based on the cropping system (e.g., Roger-Estrade et al., 2000) could then be used to calculate the proportion of compacted soil zones and derive the 1D_DPERM parameters to implement in the crop model. In a Br^- breakthrough curve experiment on a soil column, Pot et al. (2005) used the 1D_DPERM and 1D_DPERM_MIM models (but in an original setup with the immobile zone in the matrix domain). Both models produced similar results close to the observed laboratory-measured data ($R^2 > 0.95$) for low and medium rainfall intensities, but the 1D_DPERM_MIM modeled the experimental data better than the other nonequilibrium transport models and supported the hypothesis of having three porous domains with two permeabilities. Although the implementation of a second domain in transport models can be challenging, it can have a large importance in describing nonequilibrium solute transport such as the pesticide fate discussed by Pot et al. (2005). For example, Filipović et al. (2016) simulated long-term wick-lysimeter water outflows from a heterogenous soil profile amended with compost using the 2D_SP model with NSE = 0.99; however, large peaks of isoproturon (*N*,*N*-dimethyl-*N*′-[4-(1-methylethyl) phenyl]urea) pesticide observed just after the application could not be simulated using the same single-porosity approach.

Importance of Subscale Soil Heterogeneity

Although many different methods of upscaling are available (Vereecken et al., 2007), their application requires some level of simplification that usually leads to neglecting local-scale nonequilibrium. These local-scale processes might have large importance for solute movement in agricultural fields where tillage and trafficking influence the topsoil structure. The presented approach reproduced preferential water flow and vertical Br^- concentration profiles and with the addition of the mobile–immobile module included subscale soil heterogeneity (embedded clods) while keeping the relation to the physical properties observed in the profile. The estimation of effective soil hydraulic parameters in heterogeneous soils remains difficult, and unique effective average properties for heterogeneous fields cannot be found for infiltration and redistribution (Ahuja et al., 2010). The field-scale soil heterogeneity can be explicitly included at the well-defined scale (e.g., compacted vs. non-compacted soil zones), while heterogeneities at the smaller local scales (e.g., compacted clods) are described by effective parameterizations and averaging (Vogel and Roth, 2003). Our approach could be a step forward in including local-scale processes proven to have a large influence on transport processes in upscaling.

Estimation of the Mass Transfer Coefficients

Many challenges still remain—for example, the determination of the exchange term parameters. While the shape and size of the compacted clods as geometry-dependent parameters can be included using detailed morphological analyses of the soil profile or from soil structure modeling (Coquet et al., 2005b; Roger-Estrade et al., 2000), more data and techniques for determining the permeability and diffusivity parameters of the various soil structures are needed. In the sensitivity analysis performed on water, α_w, and solute, α_s, transfer rate coefficients, large variations in the final vertical concentration profiles were found. Previous research (e.g., Ellerbrock and Gerke, 2004; Leue et al., 2018) has indicated the influence of different properties of the matrix–fracture interface (e.g., hydraulic conductivity, sorption, organic matter content), which may cause local non-equilibrium conditions. Quantification of the mass transfer effects in larger scale modeling (e.g., plot, field) remains challenging. Interface properties between two porous domains can be identified from X-ray computed tomography images (Gerke, 2012) but information is still limited. Simulations with various shapes of soil structures from profile observations (e.g., embedded clods) might enlighten their influence on overall transport processes including mass exchange between pore domains.

Conclusions

The water and tracer (Br^-) distribution data from a field experiment that accounted for field spatial heterogeneity of soil hydraulic and transport processes originating from tillage and trafficking was reproduced using a two-dimensional single-porosity model (2D_SP). The two-dimensional model outputs served to test one-dimensional dual-region flow models, i.e., 1D_DPERM and 1D_DPERM with MIM. The idea was to include structural heterogeneities in 1D vertical flow models in the form of effective parameters. The application of the concept of reducing spatial dimensionality by introducing effective parameters suggested that within-field soil heterogeneities could be accounted for in 1D dual-region models of water and solute transport at the plot scale using dual-permeability modeling. Additionally, this approach allowed the inclusion of a subscale soil heterogeneous structure in a 1D model with the implementation of the mobile–immobile water

(MIM) concept. While the size and shape characteristics as well as the volume of the matrix (compacted) vs. fracture (non-compacted) domains affected the simulation results, exchange coefficients for water and solute mass transfer proved to be the major issue because its sensitivity strongly influenced the Br^- concentration profiles. Challenges remain in better estimation of the mass transfer coefficients at the matrix–fracture interface and in the upscaling of such complex interactions at larger (field) scales.

Acknowledgments

We acknowledge the traveling funding between Croatia (MZOS) and Germany (DAAD, Project SLOPE_FLOW under Grant Contract 57217986) and PHC COGITO 2015/2017 bilateral research agreement (Contract 33049VJ/37472QB) between France and Croatia, which contributed to this work. We acknowledge support by the Open Access Publication Fund of the University of Zagreb, Faculty of Agriculture.

References

Ahuja, L.R., L. Ma, and T.R. Green. 2010. Effective soil properties of heterogeneous areas for modeling infiltration and redistribution. Soil Sci. Soc. Am. J. 74:1469–1482. doi:10.2136/sssaj2010.0073

Arora, B., B.P. Mohanty, and J.T. McGuire. 2015. An integrated Markov chain Monte Carlo algorithm for upscaling hydrological and geochemical parameters from column to field scale. Sci. Total Environ. 512–513:428–443. doi:10.1016/j.scitotenv.2015.01.048

Cadini, F., J. De Sanctis, I. Bertoli, and E. Zio. 2012. Upscaling of a dual-permeability Monte Carlo simulation model for contaminant transport in fractured networks by genetic algorithm parameter identification. Stochastic Environ. Res. Risk Assess. 27:505–516. doi:10.1007/s00477-012-0595-8

Coquet, Y., C. Coutadeur, C. Labat, P. Vachier, M.Th. van Genuchten, J. Roger-Estrade, and J. Šimůnek. 2005a. Water and solute transport in a cultivated silt loam soil: 1. Field observations. Vadose Zone J. 4:573–586. doi:10.2136/vzj2004.0152

Coquet, Y., C. Coutadeur, C. Labat, P. Vachier, M.Th. van Genuchten, J. Roger-Estrade, and J. Šimůnek. 2005b. Water and solute transport in a cultivated silt loam soil: 2. Numerical analysis. Vadose Zone J. 4:587–601. doi:10.2136/vzj2004.0153

Ellerbrock, R.H., and H.H. Gerke. 2004. Characterizing organic matter of soil aggregate coatings and biopores by Fourier transform infrared spectroscopy. Eur. J. Soil Sci. 55:219–228. doi:10.1046/j.1365-2389.2004.00593.x

Ellsworth, T.R., and W.A. Jury. 1991. A three-dimensional field study of solute transport through unsaturated, layered, porous media: 2. Characterization of vertical dispersion. Water Resour. Res. 27:967–981. doi:10.1029/91WR00190

Filipović, V., Y. Coquet, V. Pot, S. Houot, and P. Benoit. 2016. Modeling water and isoproturon dynamics in a soil profile with different urban waste compost application considering local heterogeneities. Geoderma 268:29–40. doi:10.1016/j.geoderma.2016.01.009

Gerke, H.H. 2006. Preferential-flow descriptions for structured soils. J. Plant Nutr. Soil Sci. 169:382–400. doi:10.1002/jpln.200521955

Gerke, H.H. 2012. Macroscopic representation on of the interface between flow domains in structured soil. Vadose Zone J. 11(3). doi:10.2136/vzj2011.0125

Gerke, H.H., J. Dusek, and T. Vogel. 2013. Solute mass transfer effects in two-dimensional dual-permeability modeling of bromide leaching from a tile-drained field. Vadose Zone J. 12(2). doi:10.2136/vzj2012.0091

Gerke, H.H., and J.M. Köhne. 2002. Estimating hydraulic properties of soil aggregate skins from sorptivity and water retention. Soil Sci. Soc. Am. J. 66:26–36. doi:10.2136/sssaj2002.2600

Gerke, H.H., and M.Th. van Genuchten. 1993a. A dual-porosity model for simulating the preferential movement of water and solutes in structured porous media. Water Resour. Res. 29:305–319. doi:10.1029/92WR02339

Gerke, H.H., and M.Th. van Genuchten. 1993b. Evaluation of a first-order water transfer term for variably saturated dual-porosity flow models. Water Resour. Res. 29:1225–1238. doi:10.1029/92WR02467

Gerke, H.H., and M.Th. van Genuchten. 1996. Macroscopic representation of structural geometry for simulating water and solute movement in dual-porosity media. Adv. Water Resour. 19:343–357. doi:10.1016/0309-1708(96)00012-7

Green, T.R., L.R. Ahuja, and J.G. Benjamin. 2003. Advances and challenges in predicting agricultural management effects on soil hydraulic properties. Geoderma 116:3–27. doi:10.1016/S0016-7061(03)00091-0

Guswa, A.J., and D.L. Freuberg. 2002. On using the equivalent conductivity to characterize solute spreading in environments with low-permeability lenses. Water Resour. Res. 38(8). doi:10.1029/2001WR000528

Gysi, M., A. Ott, and H. Flühler. 1999. Influence of single passes with high wheel load on a structured, unploughed sandy loam soil. Soil Tillage Res. 52:141–151. doi:10.1016/S0167-1987(99)00066-5

Hansen, H.C.B., M.B. Jensen, and J. Magid. 1999. Phosphate sorption to matrix and fracture wall materials in a Glossaqualf. Geoderma 90:243–261. doi:10.1016/S0016-7061(98)00126-8

Haws, N.W., P.S.C. Rao, J. Šimůnek, and I.C. Poyer. 2005. Single-porosity and dual-porosity modeling of water flow and solute transport in subsurface drained fields using effective field-scale parameters. J. Hydrol. 313:257–273. doi:10.1016/j.jhydrol.2005.03.035

Ippisch, O., H.-J. Vogel, and P. Bastian. 2006. Validity limits for the van Genuchten–Mualem model and implications for parameter estimation and numerical simulation. Adv. Water Resour. 29:1780–1789. doi:10.1016/j.advwatres.2005.12.011

Jacques, D., J. Šimůnek, A. Timmerman, and J. Feyen. 2002. Calibration of Richards' and convection–dispersion equations to field-scale water flow and solute transport under rainfall conditions. J. Hydrol. 259:15–31. doi:10.1016/S0022-1694(01)00591-1

Jarvis, N.J. 2007. A review of non-equilibrium water flow and solute transport in soil macropores: Principles, controlling factors and consequences for water quality. Eur. J. Soil Sci. 58:523–546. doi:10.1111/j.1365-2389.2007.00915.x

Jensen, K.H., and J.C. Refsgaard. 1991. Spatial variability of physical parameters and processes in two field soils: II. Water flow at field scale. Hydrol. Res. 22:303–326. doi:10.2166/nh.1991.0021

Köhne, J.M., H.H. Gerke, and S. Köhne. 2002. Effective diffusion coefficients of soil aggregates with surface skins. Soil Sci. Soc. Am. J. 66:1430–1438. doi:10.2136/sssaj2002.1430

Lai, J., and L. Ren. 2016. Estimation of effective hydraulic parameters in heterogeneous soils at field scale. Geoderma 264:28–41. doi:10.1016/j.geoderma.2015.09.013

Leue, M., A. Wohld, and H.H. Gerke. 2018. Two-dimensional distribution of soil organic carbon at intact macropore surfaces in BT-horizons. Soil Tillage Res. 176:1–9. doi:10.1016/j.still.2017.10.002

Mallants, D., D. Jacques, M. Vanclooster, J. Diels, and J. Feyen. 1996. Stochastic approach to simulate water flow in a macroporous soil. Geoderma 70:299–324. doi:10.1016/0016-7061(95)00084-4

Mayer, S., T.R. Ellsworth, D.L. Corwin, and K. Loague. 1999. Identifying effective parameters for solute transport models in heterogeneous environments. In: D.L. Corwin et al., editors, Assessment of non-point source pollution in the vadose zone. Am. Geophys. Union, Washington, DC. p. 119–133. doi:10.1029/GM108p0119

Moeys, J., M. Larsbo, L. Bergström, C.D. Brown, Y. Coquet, and N.J. Jarvis. 2012. Functional test of pedotransfer functions to predict water flow and solute transport with the dual-permeability model MACRO. Hydrol. Earth Syst. Sci. 9:2245–2282. doi:10.5194/hessd-9-2245-2012

Mohanty, B.P., M.D. Ankeny, R. Horton, and R.S. Kanwar. 1994. Spatial analysis of hydraulic conductivity measured using disc infiltrometers. Water Resour. Res. 30:2489–2498. doi:10.1029/94WR01052

Nash, J.E., and J.V. Sutcliffe. 1970. River flow forecasting through conceptual models: I. A discussion of principles. J. Hydrol. 10:282–290. doi:10.1016/0022-1694(70)90255-6

Petersen, C.T., H.E. Jensen, S. Hansen, and C. Bender Koch. 2001. Susceptibility of a sandy loam soil to preferential flow as affected by tillage. Soil Tillage Res. 58:81–89. doi:10.1016/S0167-1987(00)00186-0

Pot, V., J. Šimůnek, P. Benoit, Y. Coquet, A. Yra, and M.-J. Martínez-Cordón. 2005. Impact of rainfall intensity on the transport of two herbicides in undisturbed grassed filter strip soil cores. J. Contam. Hydrol. 81:63–88. doi:10.1016/j.jconhyd.2005.06.013

Roger-Estrade, J., G. Richard, H. Boizard, J. Boiffin, J. Caneill, and H. Manichon. 2000. Modelling structural changes in tilled topsoil over time as a function of cropping systems. Eur. J. Soil Sci. 51:455–474. doi:10.1046/j.1365-2389.2000.00323.x

Schneider, S., Y. Coquet, P. Vachier, C. Labat, J. Roger-Estrade, P. Benoit, et al. 2009. Effect of urban waste compost application on soil near-saturated hydraulic conductivity. J. Environ. Qual. 38:772–781. doi:10.2134/jeq2008.0098

Šimůnek, J., and M.Th. van Genuchten. 2008. Modeling nonequilibrium flow and transport processes using HYDRUS. Vadose Zone J. 7:782–797. doi:10.2136/vzj2007.0074

Šimůnek, J., M.Th. van Genuchten, and M. Šejna. 2016. Recent developments and applications of the HYDRUS computer software packages. Vadose Zone J. 15(7). doi:10.2136/vzj2016.04.0033

Smith, R.E., and B. Diekkrüger. 1996. Effective soil water characteristics and ensemble soil water profiles in heterogeneous soils. Water Resour. Res. 32:1993–2002. doi:10.1029/96WR01048

Vanderborght, J., M. Vanclooster, A. Timmerman, P. Seuntjens, D. Mallants, D.J. Kim, et al. 2001. Overview of inert tracer experiments in key Belgian soil types: Relation between transport and soil morphological and hydraulic properties. Water Resour. Res. 37:2873–2888. doi:10.1029/2000WR000110

Vereecken, H., R. Kasteel, J. Vanderborght, and T. Harter. 2007. Upscaling hydraulic properties and soil water flow processes in heterogeneous soils: A review. Vadose Zone J. 6:1–28. doi:10.2136/vzj2006.0055

Vereecken, H., A. Schnepf, J.W. Hopmans, M. Javaux, D. Or, T. Roose, et al. 2016. Modeling soil processes: Review, key challenges, and new perspectives. Vadose Zone J. 15(5). doi:10.2136/vzj2015.09.0131

Vieublé-Gonod, L., P. Benoit, N. Cohen, and S. Houot. 2009. Spatial and temporal heterogeneity of soil microorganisms and isoproturon degrading activity in a tilled soil in relation to urban waste compost application. Soil Biol. Biochem. 41:2558–2567. doi:10.1016/j.soilbio.2009.09.017

Vogel, T., H.H. Gerke, R. Zhang, and M.Th. van Genuchten. 2000a. Modeling flow and transport in a two-dimensional dual-permeability system with spatially variable hydraulic properties. J. Hydrol. 238:78–89. doi:10.1016/S0022-1694(00)00327-9

Vogel, H.J., and K. Roth. 2003. Moving through scales of flow and transport in soil. J. Hydrol. 272:95–106. doi:10.1016/S0022-1694(02)00257-3

Vogel, T., M.Th. van Genuchten, and M. Cislerova. 2000b. Effect of the shape of the soil hydraulic functions near saturation on variably-saturated flow predictions. Adv. Water Resour. 24:133–144. doi:10.1016/S0309-1708(00)00037-3

Wang, W., S.P. Neuman, T. Yao, and P.J. Wierenga. 2003. Simulation of large-scale field infiltration experiments using a hierarchy of models based on public, generic, and site data. Vadose Zone J. 2:297–312. doi:10.2136/vzj2003.2970

Zhang, Z.F., A.L. Ward, and G.W. Gee. 2004. A combined parameter scaling and inverse technique to upscale the unsaturated hydraulic parameters for heterogeneous soils. Water Resour. Res. 40:W08306. doi:10.1029/2003WR002925

Zhu, J., and B.P. Mohanty. 2002. Upscaling of soil hydraulic properties for steady state evaporation and infiltration. Water Resour. Res. 38(9):1178. doi:10.1029/2001WR000704

Zhu, J., and B.P. Mohanty. 2003. Effective hydraulic parameters for steady state vertical flow in heterogeneous soils. Water Resour. Res. 39:1227. doi:10.1029/2002WR001831